CMOS image sensors based on linear mode APDs: analysis and future perspectives

Lucio Pancheri[a], Olga Shcherbakova[a,b], Nicola Massari[b], Gian-Franco Dalla Betta[a] and David Stoppa[b]

[a]*University of Trento, Via Sommarive, 14, 38123 Trento, Italy*
[b]*Fondazione Bruno Kessler, Via Sommarive, 18, 38123 Trento, Italy*
phone: +39 0461 281532, e-mail: lucio.pancheri@unitn.it

ABSTRACT

This paper presents the experimental noise characteristics of avalanche photodiodes (APDs) fabricated in different CMOS technologies, showing the possibility to achieve a low noise factor as a consequence of dead-space effect. The example application of a CMOS range image sensor based on gain-modulated APDs is presented and the perspectives for a future development of APD image sensors are discussed.

INTRODUCTION

A decade after the demonstration of the first monolithic Geiger-mode Avalanche Photodiode (APD) arrays, the scientific and industrial communities are becoming increasingly interested in the potential of this technology. What has been mostly unexplored so far is the use of APDs operating in the sub-Geiger regime in image sensor pixels. Although an early attempt to fabricate CMOS APD pixel arrays was done in the early 2000s [1], the results obtained were not encouraging enough to push further research efforts in that direction. The main problem of this first attempt was the high noise factor of the detector, arising from hole-triggered avalanche multiplication. Since then, several studies on CMOS linear APDs have been published, demonstrating that APDs with reasonably low noise factors were feasible in standard CMOS technologies [2 – 4]. In addition, deep-submicron CMOS devices with increasingly good characteristics in the Geiger mode have been developed [5], making it worth reconsidering the study of image sensors based on linear-mode APDs.
In this paper, the noise characteristics of three different APDs fabricated in different CMOS technologies are analyzed and the possibilities and issues offered by the integration of sub-Geiger APD image sensors are critically discussed. Finally, some results from the characterization of a Time-of-Flight (ToF) range camera based on gain-modulated APDs are presented.

DEVICE CHARACTERISTICS

The schematic cross section of three APDs fabricated in different technology nodes is shown in Figure 1. Although the structures are slightly different, in all three cases the avalanche region consists of a p^+/nwell junction. The three APDs break down at different voltages: 20.8V, 16V and 10.8V, as a result of different nwell doping concentrations. Figure 2 shows the multiplication gain of the three devices as a function of reverse bias voltage. The experimental noise factors are reported in Figures 3-5, both under UV light illumination and at longer wavelengths, to take into account both the case of pure electron injection and that of a dominant hole injection. For reference, noise factors simulated with the standard McIntyre theory are also reported. While a reasonably good agreement is found for APD A, having the highest breakdown voltage, the experimental noise for the other two devices is significantly lower than the simulated one. This difference between experimental and theoretical noise can be attributed to dead-space effect [6], which becomes increasingly important as the thickness of the multiplication region is reduced.
The noise factor of APDs B and C is small enough to be exploited in several application domains. Apart from optical communications, they could be usefully employed in imaging applications requiring high speed and high sensitivity such as optical ranging, scintillator readout and ultra-high-speed imaging. In these applications, pixels must have a large area due to the required high sensitivity, while the high bandwidth of the output signal chain causes the readout noise to be typically larger than in ordinary image sensors. With these conditions, the fill factor reduction due to the

unavoidable guard ring can be tolerated and the benefits of multiplication gain are only partially spoiled by the moderate avalanche noise factor.
An estimation of the pixel SNR based on the parameters of APD C is reported in Figure 6, showing a relevant SNR increase at small signal levels when a moderate gain M = 5 or M = 10 is applied. In this simulation, a readout noise of 50 electrons was considered, which can be representative of the noise of a large pixel, in the order of 10s of µm.
Another fundamental aspect to be taken into account is the presence of tunneling dark current that would increase with the peak electric field, and could badly affect the noise floor of the device. In the presence of a high-speed readout, however, the added noise due to an increased dark current could still be negligible with respect to electronics readout noise.

APD RANGE CAMERA

As an application example, a 64x64-pixel array range camera based on APD C operated in linear mode is briefly reported [7]. Figure 7 illustrates the operation principle of the Time-of-Flight demodulation pixel used: APD voltage modulation is used to obtain photocurrent gain modulation, and therefore phase-sensitive detection.
To operate in this regime, the in-pixel electronic readout channel must assure a stable bias voltage operation and the possibility of modulating the APD cathode. A low-bandwidth in-pixel charge amplifier was implemented to meet these requirements and assure a low power consumption (Figure 8). An additional input capacitance was used to stabilize the input node at the high modulation frequencies used in ToF ranging applications. The pixel has 30µm pitch with 25.7% fill factor and 10fF integration capacitance.
The imager features a good breakdown voltage uniformity, a current consumption lower than 15mA and a dynamic range of 50.5dB at M = 10. Thanks to the high APD bandwidth, a state-of-the-art demodulation contrast as a function of bias voltage was obtained on single pixels, reaching a maximum value of 80% at 200MHz, as reported in Figure 9. A range image is shown in Figure 10, together with its histogram and the demodulated signal intensity image.

CONCLUSION

The analysis of the noise characteristics of APDs fabricated in different CMOS technologies shows that a low noise factor can be achieved, opening the way for the use of linear mode APDs in imaging applications requiring high sensitivity and high speed readout. The implementation of a ToF range camera based on gain-modulated APDs is a first demonstration of the approach feasibility. Although the proposed design needs to be optimized under several points of view to rival the performance of the best commercial 3D cameras, the potential for a future development of this concept appears clear and justifies further research efforts in this direction.

REFERENCES

[1] A. Biber et al., “Avalanche photodiode image sensor in standard BiCMOS technology”, IEEE Trans. Electron Devices, vol. 47, no. 11, pp. 2241–2243, Nov. 2000.
[2] A. Rochas et al., “Low-noise silicon avalanche photodiodes fabricated in conventional CMOS technologies”, IEEE Trans. Electron Dev., vol. 49, no. 3, pp. 387–394, Mar. 2002.
[3] L. Pancheri, et al. “Low-noise avalanche photodiode in standard 0.35-µm CMOS technology”, IEEE Trans. Electron Devices, vol. 55, no. 1, pp. 457-461, Jan. 2008.
[4] M. Atef, et al., “Avalanche double photodiode in 40-nm standard CMOS technology”, IEEE J. Quantum Electron., vol. 49, no. 3, pp. 350–356, Mar. 2013.
[5] J.A. Richardson et al., “Scaleable Single-Photon Avalanche Diode structures in nanometer CMOS technology”, IEEE Trans. Electron Devices, vol. 58, no. 7, pp. 2028 – 2035, 2011.
[6] A.R. Pauchard et al., “Dead space effect on the wavelength dependence of gain and noise in avalanche photodiodes”, IEEE Trans. Electron Devices, vol. 47, no. 9, pp. 1685–1693, Sep. 2000.
[7] O. Shcherbakova et al., “3D camera based on linear-mode gain-modulated avalanche photodiodes”, ISSCC Dig. Tech. Papers, pp. 490-491, 2013.

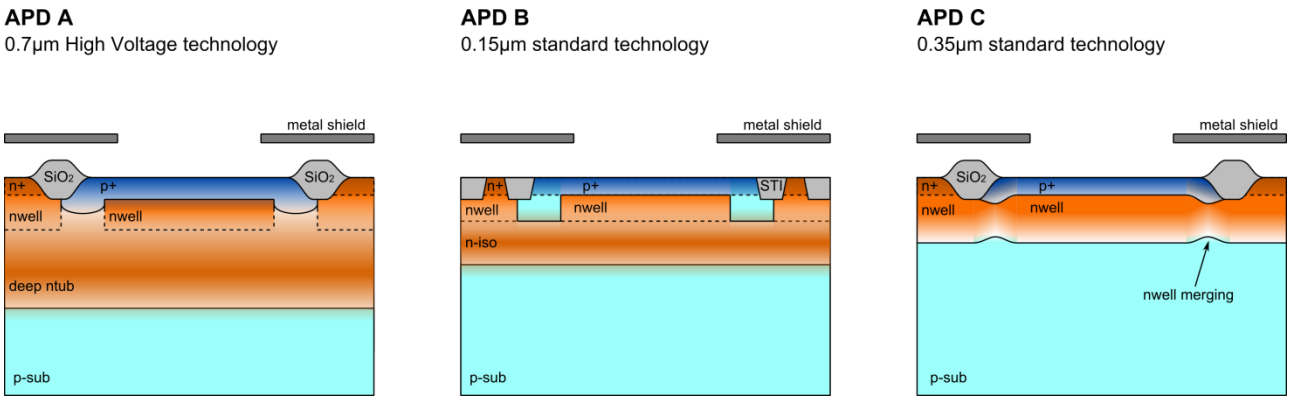

Figure 1. Schematic cross-sectional views of three APDs fabricated in different technologies.

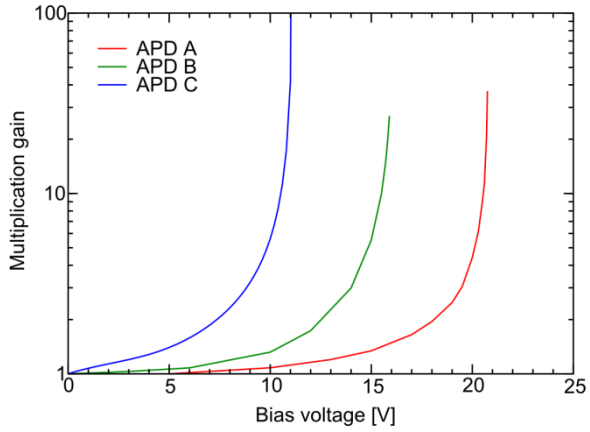

Figure 2. APD multiplication gain as a function of bias voltage

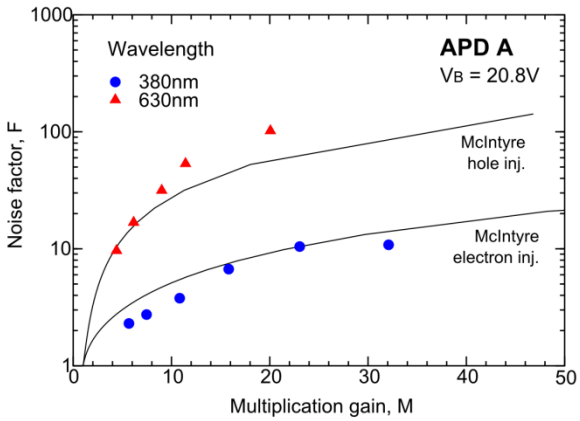

Figure 3. Experimental and simulated noise factor as a function of gain for APD A

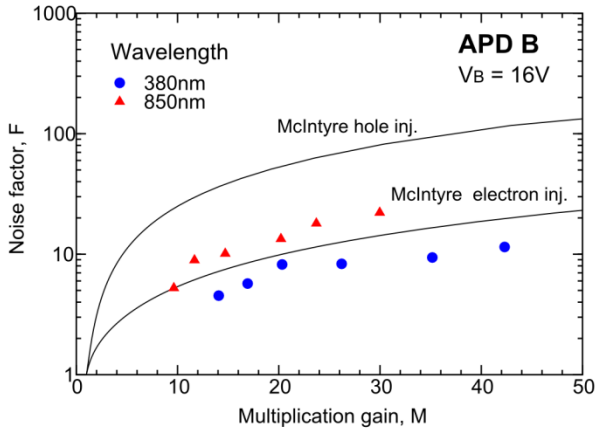

Figure 4. Experimental and simulated noise factor as a function of gain for APD B

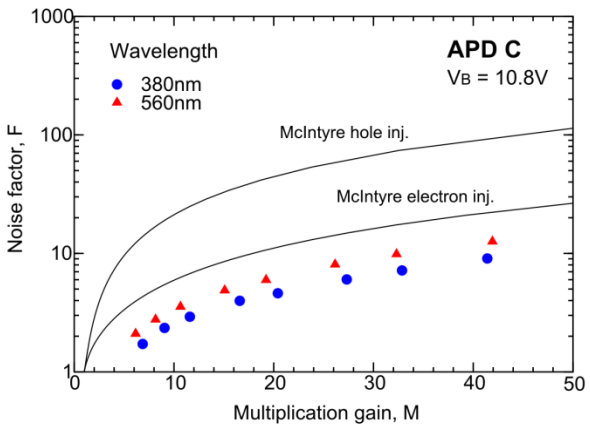

Figure 5. Experimental and simulated noise factor as a function of gain for APD C

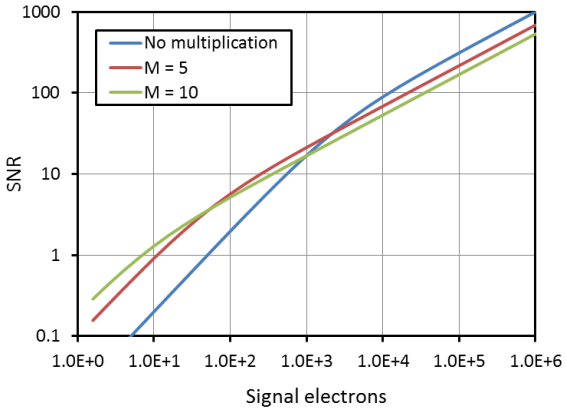

Figure 6. Simulated SNR of APD C at different values of gain for an electronic readout noise of 50 electrons

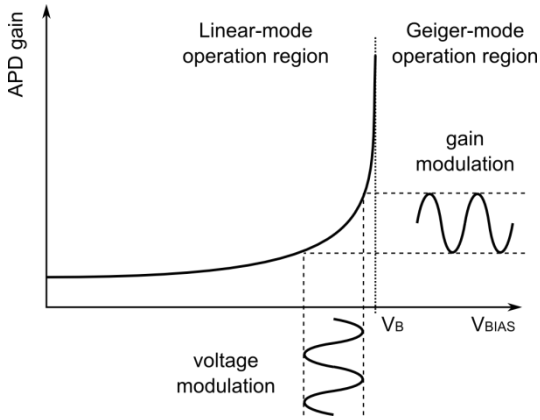

Figure 7. APD gain modulation used in phase-sensitive light detection

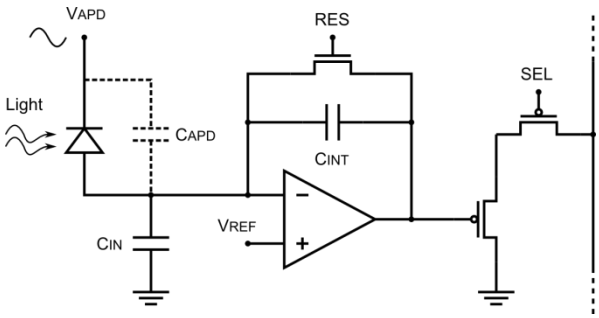

Figure 8. Pixel schematic assuring constant bias operation and gain modulation

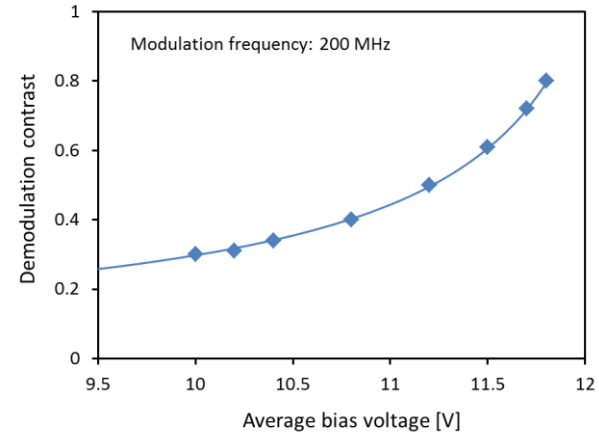

Figure 9. Demodulation contrast measured at 200 MHz modulation frequency. The illumination source was a red laser (650nm). Square wave modulation was used.

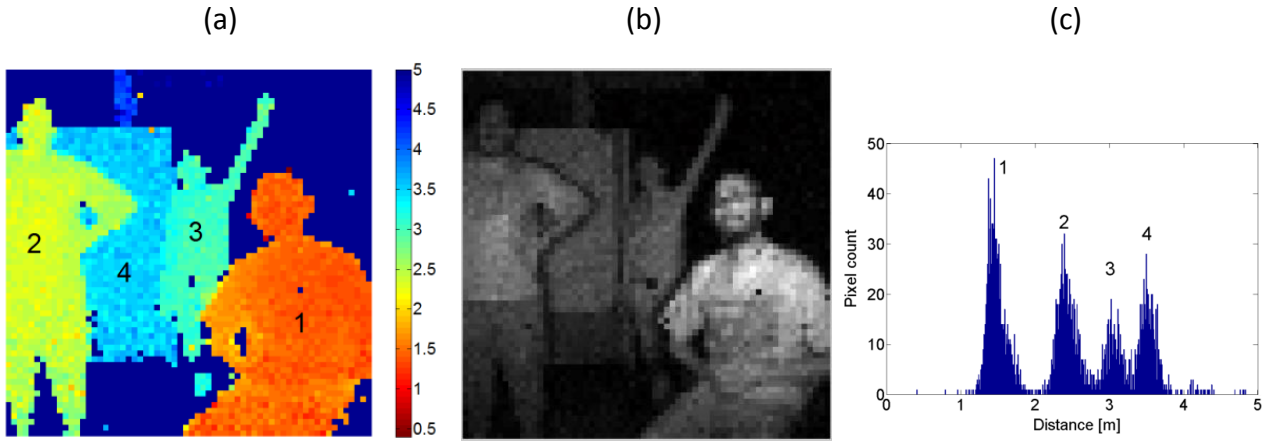

Figure 10. Sample image extracted from a video sequence at 50fps: (a) Range image (b) Demodulated signal intensity image (c) Range image histogram. A high power LED-based IR illumination module modulated at 25 MHz was used.